NASA TECHNICAL NOTE

NASA TN D-8317

NASA TN D-8317 c.3

c.1

ISOTHERMAL ELASTOHYDRODYNAMIC LUBRICATION OF POINT CONTACTS

III - Fully Flooded Results

Bernard J. Hamrock and Duncan Dowson

Lewis Research Center
Cleveland, Ohio 44135

NATIONAL AERONAUTICS AND SPACE ADMINISTRATION • WASHINGTON, D. C. • OCTOBER 1976

1. Report No. NASA TN D-8317	2. Government Accession No.	3. Recipient's Catalog No.
4. Title and Subtitle ISOTHERMAL ELASTOHYDRODYNAMIC LUBRICATION OF POINT CONTACTS III - FULLY FLOODED RESULTS		5. Report Date October 1976 6. Performing Organization Code
7. Author(s) Bernard J. Hamrock of the Lewis Research Center; and Duncan Dowson of the University of Leeds		8. Performing Organization Report No. E-8712
9. Performing Organization Name and Address Lewis Research Center National Aeronautics and Space Administration Cleveland, Ohio 44135		10. Work Unit No. 505-04 11. Contract or Grant No.
12. Sponsoring Agency Name and Address National Aeronautics and Space Administration Washington, D.C. 20546		13. Type of Report and Period Covered Technical Note 14. Sponsoring Agency Code

15. Supplementary Notes

16. Abstract

The theory developed by the authors in an earlier publication was used to investigate the influence of the ellipticity parameter and the dimensionless speed U, load W, and material G parameters on minimum film thickness. The ellipticity parameter k was varied from 1 (a ball-on-plate configuration) to 8 (a configuration approaching a line contact). The dimensionless speed parameter was varied over a range of nearly two orders of magnitude. And the dimensionless load parameter was varied over a range of one order of magnitude. Conditions corresponding to the use of solid materials of bronze, steel, and silicon nitride and lubricants of paraffinic and naphthenic mineral oils were considered in obtaining the exponent on the dimensionless material parameter. Thirty-four different cases were used in obtaining the minimum-film-thickness formula $\tilde{H}_{min} = 3.63\ U^{0.68} G^{0.49} W^{-0.073} (1 - e^{-0.68k})$. A simplified expression for the ellipticity parameter $k = 1.03\ (R_y/R_x)^{0.64}$ can be written, where R_y/R_x is the radius of curvature ratio. Contour plots are also shown that indicate in detail the pressure spike and the two side lobes in which the minimum film thickness occurs. These theoretical solutions of film thickness have all the essential features of previously reported experimental observations based upon optical interferometry.

17. Key Words (Suggested by Author(s)) Elastohydrodynamics Lubrication Bearings Gears	18. Distribution Statement Unclassified - unlimited STAR Category 37

19. Security Classif. (of this report) Unclassified	20. Security Classif. (of this page) Unclassified	21. No. of Pages 39	22. Price* $4.00

* For sale by the National Technical Information Service, Springfield, Virginia 22161

ISOTHERMAL ELASTOHYDRODYNAMIC LUBRICATION OF POINT CONTACTS

III - FULLY FLOODED RESULTS*

by Bernard J. Hamrock and Duncan Dowson†

Lewis Research Center

SUMMARY

The theory developed by the authors in an earlier publication was used to investigate the influence of the ellipticity parameter and the dimensionless speed U, load W, and material parameters on minimum film thickness. The ellipticity parameter was varied from 1 (a ball-on-plate configuration) to 8 (a configuration approaching a line contact). The dimensionless speed parameter was varied over a range of nearly two orders of magnitude. And the dimensionless load parameter was varied over a range of one order of magnitude. Conditions corresponding to the use of solid materials of bronze, steel, and silicon nitride and lubricants of paraffinic and naphthenic mineral oils were considered in obtaining the exponent on the dimensionless material parameter. Thirty-four different cases were used in obtaining the minimum-film-thickness formula

$$\tilde{H}_{min} = 3.63\, U^{0.68} G^{0.49} W^{-0.073} (1 - e^{-0.68k})$$

A simplified expression for the ellipticity parameter k was found, where

$$k = 1.03\left(\frac{R_y}{R_x}\right)^{0.64}$$

R_y/R_x being the radius of curvature ratio.

Contour plots are also shown that indicate in detail the pressure spike and the two side lobes in which the minimum film thickness occurs. These theoretical solutions of film thickness have all the essential features of previously reported experimental observations based upon optical interferometry.

*Presented at Joint Lubrication Conference cosponsored by the American Society of Mechanical Engineers and the American Society of Lubrication Engineers, Boston, Massachusetts, October 5-7, 1976.

†Professor of Mechanical Engineering, University of Leeds, Leeds, England.

INTRODUCTION

Only in recent years has the complete theoretical solution of the isothermal elastohydrodynamic lubrication (EHL) of point contacts been successfully analyzed. The analysis requires the simultaneous solution of the elasticity and Reynolds equations. The authors' approach to the theoretical solution has been presented in two previous publications (refs. 1 and 2). The first of these publications (ref. 1) presents the elasticity model in which the conjunction is divided into equal rectangular areas with a uniform pressure applied over each area. The second (ref. 2) gives the complete approach to solving the elastohydrodynamic lubrication problem for point contacts.

The most important practical aspect of the EHL point-contact theory (ref. 2) is the determination of the minimum film thickness within the contact. That is, maintaining a fluid film thickness of adequate magnitude is extremely important to the operation of some machine elements. In the present report, only the results from the theory given in references 1 and 2 are presented. In the results the influence of contact geometry as expressed in the ellipticity parameter and the dimensionless speed, load, and material parameters on minimum film thickness is investigated for a conjunction fully immersed in lubricant (i.e., fully flooded). The ellipticity results have been presented in reference 3 by the authors, but in the present report additional solutions are presented and the accuracy of the presentation is improved. The corrected ellipticity results are presented in this report. In the numerical work the ellipticity parameter was varied from 1 (a ball-on-plate configuration) to 8 (a configuration approaching a line contact). The dimensionless speed and load parameters were varied over ranges of about two and one orders of magnitude, respectively. Conditions equivalent to using solid materials of bronze, steel, and silicon nitride and lubricants of paraffinic and naphthenic mineral oils were considered in obtaining the exponent on the dimensionless material parameter. Thirty-four different cases were used in obtaining the fully flooded film-thickness formulas. A fully flooded condition is said to exist when the inlet distance of the conjunction ceases to influence, in any significant way, the minimum film thickness. The inlet distance of the conjunction is defined as the distance from the center of the contact to the edge of the computing area. Contour plots are also shown that indicate in detail the pressure spike and the two side lobes in which the minimum film thickness occurs.

SYMBOLS

a semimajor axis of contact ellipse

b semiminor axis of contact ellipse

D_1 $\left(\frac{\tilde{H}_{min} - H_{min}}{H_{min}}\right)100$

D_2 $\left(\frac{\tilde{H}_c - H_c}{H_c}\right)100$

E modulus of elasticity

E' $\frac{2}{\left(\frac{1 - \nu_A^2}{E_A} + \frac{1 - \nu_B^2}{E_B}\right)}$

F normal applied load

G dimensionless material parameter, $E'/p_{iv,as}$

H dimensionless film thickness, h/R_x

H_c dimensionless central film thickness obtained from EHL point-contact theory (ref. 2)

$\tilde{H}_c$ dimensionless central film thickness obtained from least-square fit of data

H_{min} dimensionless minimum film thickness obtained from EHL point-contact theory (ref. 2)

$\tilde{H}_{min}$ dimensionless minimum film thickness obtained from least-square fit of data

$H_{min,L}$ dimensionless minimum film thickness for line contact

h film thickness

k ellipticity parameter, a/b

P dimensionless pressure, p/E'

p pressure

$p_{iv,as}$ asymptotic isoviscous pressure

R effective radius

r radius of curvature

U dimensionless speed parameter, $u\eta_o/E'R_x$

u surface velocity in x-direction

W dimensionless load parameter, $F/E'R_x^2$

$x, X, \overline{X}$
$y, Y, \overline{Y}$ } coordinate systems defined in report

α pressure-viscosity coefficient

η_o atmospheric viscosity

ν Poisson's ratio

Subscripts:

A solid A

B solid B

x,y coordinates system defined in report

DIMENSIONLESS GROUPING

From the variables of the numerical analysis (ref. 2) the following dimensionless groups can be defined:

(1) Dimensionless film thickness

$$H = \frac{h}{R_x} \tag{1}$$

(2) Ellipticity parameter

$$k = \frac{a}{b} \tag{2}$$

(3) Dimensionless speed parameter

$$U = \frac{\eta_o u}{E' R_x} \tag{3}$$

(4) Dimensionless load parameter

$$W = \frac{F}{E' R_x^2} \tag{4}$$

(5) Dimensionless material parameter

$$G = \frac{E'}{p_{iv,as}} \tag{5}$$

where $p_{iv,as}$ is the asymptotic isoviscous pressure obtained from Roelands (ref. 4). The asymptotic isoviscous pressure can be approximated by the inverse of the pressure-viscosity coefficient ($p_{iv,as} \approx 1/\alpha$).

The dimensionless film thickness can be written as

$$H = f(k, U, W, G) \tag{6}$$

The most important practical aspect of the EHL point-contact theory developed in reference 2 is the determination of the minimum film thickness within the conjunction. Therefore, in the fully flooded results presented herein the dimensionless parameters (k, U, W, and G) will be varied and the effect upon minimum film thickness will be studied.

Effect of Ellipticity of Elastic Conjunction

The ellipticity parameter k is a function of the radii of curvature of the solids only (r_{Ax}, r_{Bx}, r_{Ay}, and r_{By}). The radii of curvature in the x-direction for both solids A and B are used in defining the dimensionless speed and load parameters. Therefore, only the radius of curvature of solid B in the y-direction was changed in varying the ellipticity parameter from 1 (a ball on-plate configuration) to 8 (a configuration approaching a line contact). In doing this the dimensionless speed U, load W, and material G parameters were held constant at the following values:

$$\left.\begin{aligned} U &= 0.1683\times10^{-11} \\ W &= 0.1106\times10^{-6} \\ G &= 4522 \end{aligned}\right\} \tag{7}$$

Care was taken to ensure that the highest ellipticity parameter (k = 8) case was in the elastic region as defined by Dowson-Higginson (p. 101, ref. 5). For ellipticity parameters less than 8 the results move farther into the elastic region.

Table I gives 10 values of the ellipticity parameter k and the corresponding minimum film thickness H_{min} as obtained from the EHL point-contact theory (ref. 2). Having these 10 pairs of data, the object was to determine an equation that describes how the ellipticity parameter affects the minimum film thickness. The general form of this equation can be written as

$$\left(1 - \frac{H_{min}}{H_{min,L}}\right) = A\, e^{Bk} \tag{8}$$

A least-square exponential curve fit to the 10 pairs of data points

$$k_i, \left(1 - \frac{H_{min}}{H_{min,L}}\right)_i \qquad \text{where } i = 1, \ldots, 10$$

was used in obtaining values for A and B in equation (8). Besides a least-square fit a coefficient of determination r^2 was obtained. The value of r^2 reflects the fit of the data to the resulting equation: 1 being a perfect fit, and zero the worst possible fit. The minimum film thickness for a line contact $H_{min,L}$ used in equation (8) was determined by finding the $H_{min,L}$ that gives a coefficient of determination closest to 1. This value of $H_{min,L}$ turned out to be 7.082×10^{-6} with a corresponding coefficient of determination of 0.9990, which is an excellent fit. Furthermore, the values of A and B in equation (8) as obtained from the least-square fit are

$$A = 0.9966 \approx 1.00 \tag{9}$$

$$B = -0.6752 \approx -0.68 \tag{10}$$

From equations (8), (9), and (10) the following equation can be written, which shows the effect of ellipticity parameter on minimum film thickness:

$$\tilde{H}_{min} \propto (1 - e^{-0.68k}) \tag{11}$$

It is most significant that A turned out to be 0.9966, or approximately 1.00, since as $k \to 0$, $H_{min} \to 0$. Therefore, even though the smallest value of k used in obtaining equation (11) was unity, it would seem that equation (11) could be applied to smaller values since in the limiting case ($k \to 0$) equation (11) satisfies the physical intuition. For the other extreme of large k, a line-contact situation is approached, and the agreement with existing results is again good. From Dowson and Higginson (ref. 5) the line-contact minimum thickness for the dimensionless parameters given in equation (7) is 7.720×10^{-6}. Compare this with 7.082×10^{-6} from the present results. The difference of 9 percent could well be the result of Dowson and Higginson (ref. 5) using an exponential pressure-viscosity relation instead of the Roelands (ref. 4) formulation used in the present work. As was pointed out in the closure of reference 2 (answering a query by P. M. Ku) the Roelands formula (ref. 4) suppresses the pressure spike somewhat and

also results in a smaller film thickness.

Substituting equations (9) and (10) into equation (8) gives $\tilde{H}_{min}$ the dimensionless minimum film thickness obtained from the least-square formulation. The $\tilde{H}_{min}$ for 10 values of the ellipticity parameter are given in table I. The percentage difference between the minimum film thickness obtained from EHL point-contact theory H_{min} and the minimum film thickness obtained from the least-square fit equation $\tilde{H}_{min}$ is expressed as

$$D_1 = \left(\frac{\tilde{H}_{min} - H_{min}}{H_{min}} \right) 100 \tag{12}$$

Note that in table I, the magnitude of D_1 is within ±3 percent for all cases.

Figures 1(a) and (b) give contour plots of dimensionless pressure for two extreme values of the ellipticity parameter k, 8 and 1.25. In these and all contour plots to be presented the + symbol indicates the center of the Hertzian contact. Note that, because of the dimensionless representation of the X- and Y-coordinates, the actual Hertzian contact ellipse becomes a circle regardless of the value of the ellipticity parameter. The Hertzian contact circle is shown in each figure by asterisks. At the top of each figure the contour labels and the corresponding values of dimensionless pressure are given. The inlet region is to the left and the exit region is to the right.

For an ellipticity parameter of 8 the maximum pressure is near the center of the contact; and, even though the conditions are in the elastic region, no pressure spike occurs. The pressure gradient at the exit end of the conjunction is much larger than that in the inlet region. For an ellipticity parameter of 1.25 a pressure spike is visible at the exit end of the contact.

Figures 2(a) and (b) show two contour plots of film thickness when the ellipticity parameter k is 8 and 1.25, respectively. For an ellipticity parameter of 8 the minimum film thickness is directly behind the axial center of the contact. For an ellipticity parameter of 1.25, two minimum-film-thickness regions occur to the sides and nearer the edge of the Hertzian circle. These results - showing the two "side lobes" in which minimum-film-thickness areas occur - produce all the essential features of previously reported experimental observations based upon optical interferometry (ref. 6).

Figures 3(a) and (b) show the variation of pressure and film thickness, respectively, in the $\bar{X}$-direction close to the midplane of the contact for three values of the ellipticity parameter. As has been true for all the ellipticity parameter results presented, the values of the dimensionless speed, load, and material parameters were held fixed as per equation (7). In figure 3(a) we find that for k = 6 no pressure spike occurs, but this well-known feature of theoretical solutions to the EHL problem is evident for k = 2.5 and k = 1.25.

In figure 3(b) for $k = 1.25$ the central region is not parallel with the $\overline{X}$-axis. The reason is probably that compressibility effects are considered in the theory (ref. 2). That is, when compressibility is considered, the film thickness in the center is reduced by the amount that the fluid volume decreases at high pressure (ref. 5).

INFLUENCE OF SPEED

By changing only the surface velocity in the x-direction u, the dimensionless speed parameter U (eq. (3)) changes, but the other dimensionless parameters (k, W, and G) remain constant. The values at which these dimensionless parameters were held constant in the calculations are

$$\left.\begin{aligned} W &= 0.7371\times10^{-6} \\ G &= 4522 \\ k &= 6 \end{aligned}\right\} \tag{13}$$

Table II gives the dimensionless speed parameter U and the corresponding minimum film thickness H_{min} as obtained from the EHL point-contact theory (ref. 2). There are 15 different values of the dimensionless speed parameter covering nearly two orders of magnitude. Having these 15 pairs of data, the objective is to determine an equation that describes how the dimensionless speed affects the minimum film thickness. The general form of this equation can be written as

$$H_{min} = IU^{J} \tag{14}$$

By applying a least-square power fit to the 15 pairs of data (U_i, $H_{min,i}$, where $i = 1, \ldots, 15$) the values of I and J were found to be

$$I = 560.18 \tag{15}$$

$$J = 0.67542 \approx 0.68 \tag{16}$$

The coefficient of determination r^2 for these results was excellent at 0.9998. Substituting equations (15) and (16) into equation (14) gives the values of $\tilde{H}_{min}$ shown in table II. The percentage difference D_1 between the minimum film thickness obtained from the EHL point-contact theory H_{min} and the minimum film thickness obtained from the least-square fit $\tilde{H}_{min}$ is expressed in equation (12) and given in table II. Note that the

variation of D_1 is less than ±2 percent.

From equations (14) and (16) the effect of dimensionless speed on dimensionless minimum film thickness can be written as

$$\tilde{H}_{min} \propto U^{0.68} \tag{17}$$

Figures 4(a) and (b) give contour plots of dimensionless pressure for two extreme values of the dimensionless speed parameter U, 0.8416×10^{-12} and 0.5050×10^{-10}. In the low-speed case ($U = 0.8416\times10^{-12}$) there is a pressure spike at the exit end of the contact. In the high-speed case ($U = 0.5050\times10^{-10}$) no pressure spike occurs. Note from figures 4(a) and (b) that the pressure in the inlet region is higher at high speeds than at low speeds.

Figures 5(a) and (b) show contour plots of dimensionless film thickness when the dimensionless speed parameter is 0.8416×10^{-12} and 0.5050×10^{-10}, respectively. In figure 5(a) the minimum film thickness appears close to the Hertzian circle and off to the side. In figure 5(b) the minimum-film-thickness area appears between the center of the contact and the Hertzian circle.

Figures 6(a) and (b) show the variation of pressure and film thickness, respectively, on the $\bar{X}$-axis near the midplane of the conjunction for three values of dimensionless speed parameter. As has been true for all the speed results, the values of the dimensionless load, material, and ellipticity parameters are held fixed as described in equation (13). In figure 6(a) the dashed line corresponds to the Hertzian pressure distribution. It can be seen from figure 6(a) that the pressure in the inlet region is higher for the high speed ($U = 0.5050\times10^{-10}$) profile. For $U = 0.8416\times10^{-11}$ the pressure spike originates very near the trailing edge of the Hertzian pressure distribution, and as the speed increases the pressure spike moves upstream. For line contacts, Dowson and Higginson (ref. 5) found results similar to those shown in figure 6(a).

The typical elastohydrodynamic film shape with an essentially parallel section in the central region is shown in figure 6(b). Also, there is a considerable change in film thickness as the dimensionless speed is changed, as indicated by equation (17). This illustrates most clearly the dominant effect of the dimensionless speed parameter upon the minimum film thickness in elastohydrodynamic contacts.

INFLUENCE OF LOAD

Changing only the normal applied load F in equation (4) causes the dimensionless load parameter W to change while the remaining dimensionless parameters (k, U, and G) remain constant. The values at which these parameters were held constant are

$$\left.\begin{aligned} U &= 0.1683\times10^{-11} \\ G &= 4522 \\ k &= 6 \end{aligned}\right\} \tag{18}$$

Table III gives the dimensionless load parameter and the corresponding minimum film thickness H_{min} as obtained from the EHL point-contact theory (ref. 2). There are eight different values of the dimensionless load parameter covering more than an order of magnitude. Having these eight pairs of data, the objective was to determine an equation that describes how the dimensionless load affects the minimum film thickness. The general form of this equation can be written as

$$H_{min} = KW^{L} \tag{19}$$

By applying a least-square power fit to the eight pairs of data (W_i, $H_{min,i}$, where $i = 1, \ldots, 8$) the values of K and L were found to be

$$K = 2.1592\times10^{-6} \tag{20}$$

$$L = -0.072924 \approx -0.073 \tag{21}$$

The coefficient of determination r^2 for these results was 0.9260, which was good but was the lowest obtained in deriving the minimum-film-thickness equation (eq. (28)). Substituting equations (20) and (21) into equation (19) gives the values of $\tilde{H}_{min}$ shown in table III. The percentage difference D_1 between the minimum film thickness obtained from the EHL point-contact theory H_{min} and the minimum film thickness obtained from the least-square fit equation $\tilde{H}_{min}$ is expressed in equation (12) and given in table III. In table III the variation of D_1 is within ±3 percent in all cases.

From equations (19) and (21) the effect of load on minimum film thickness can be written as

$$\tilde{H}_{min} \propto W^{-0.073} \tag{22}$$

Figures 7(a) and (b) give contour plots of dimensionless pressure for the two extreme values of dimensionless load parameter W that were investigated, 0.1106×10^{-6} and 0.1290×10^{-5}. No pressure spike is evident at the lowest load, but at the highest load a pressure spike is visible.

Contour plots of dimensionless film thickness for the same two values of dimension-

less load parameter as given in figure 7 are shown in figure 8. In figure 8(a) for the low-load case ($W = 0.1106\times10^{-6}$) the minimum film thickness occurs directly behind the center of the contact. In figure 8(b) for the high-load case ($W = 0.1290\times10^{-5}$) the minimum film thickness is off to the sides in two areas close to the Hertzian circle.

The variation of pressure and film thickness in the $\overline{X}$-direction along a line close to the midplane of the conjunction is shown in figure 9 for three values of the dimensionless load parameter. The values of the dimensionless speed, material, and ellipticity parameters were held fixed as described by equation (18) for all computations at various loads. In figure 9(a) as the dimensionless load is increased the inlet pressure becomes smaller. For the highest load case shown in figure 9(b), film thickness rises between the central region and the outlet restriction in the same manner as seen in figure 3(b). Again this is attributed to the compressibility effects of the fluid. Also, at a load W of 0.5528×10^{-6} the film thickness is slightly smaller than at a W of 1.106×10^{-6}. The reason is that the minimum film thickness is closer to the axial center of the contact at the lower load than at the higher load. As was pointed out in discussing figures 8(a) and (b), the location of the minimum-film-thickness region changes as the dimensionless load is changed.

EFFECT OF MATERIAL PROPERTIES

The effect of the dimensionless material parameter on minimum film thickness is not a simple matter. As can be seen from equations (3), (4), and (5), when either the material of the solids (as expressed in E') or the material of the lubricant (as expressed in η_o and $p_{iv,as}$) is varied, not only does the material parameter G change, but so do the dimensionless speed U and load W parameters. Only the ellipticity parameter can be held fixed. For all the results presented in this section the ellipticity parameter is held fixed at 6.

Table IV gives the four material-parameter results. The general form showing how the minimum film thickness is a function of the dimensionless material parameter is given as

$$C = TG^{V} \tag{23}$$

where

$$C = \frac{H_{min}}{(1 - e^{-0.68k})U^{0.68}W^{-0.073}} \tag{24}$$

In equation (24) the exponents are rounded off to two significant figures so that any error could be absorbed in T given in equation (23). By applying a least-square power fit to the four pairs of data, the values of T and V were found to be

$$T = 3.6891 \tag{25}$$

$$V = 0.48669 \approx 0.49 \tag{26}$$

The coefficient of determination for these results was 0.9980, which is excellent. Substituting equations (25) and (26) into equation (23) gives the values of $\tilde{H}_{min}$ shown in table IV. The percentage difference D_1 shown in table IV varies by less than 2 percent in all cases. Therefore, from equations (23) and (25) the effect of the dimensionless material parameter on the dimensionless film thickness can be written as

$$\tilde{H}_{min} \propto G^{0.49} \tag{27}$$

MINIMUM-FILM-THICKNESS FORMULA

The proportionality expressions (11), (17), (22), and (27) established how the minimum film thickness varies with the ellipticity, speed, load, and material parameters, respectively. This enables a composite minimum-film-thickness formula for a fully flooded, isothermal, elastohydrodynamic point contact to be written as

$$\tilde{H}_{min} = 3.63\, U^{0.68} G^{0.49} W^{-0.073} \left(1 - e^{-0.68k}\right) \tag{28}$$

In equation (28) the constant 3.63 is different from that in equation (25) to account for rounding off the material-parameter exponent.

Table V gives the 34 different cases used in obtaining equation (28). In this table, H_{min} corresponds to the minimum film thickness obtained from the EHL point-contact theory developed in reference 2, and $\tilde{H}_{min}$ is the minimum film thickness obtained from equation (28). The percentage difference between these two values is expressed by D_1, which is defined in equation (12). In table V the values of D_1 are within ±5 percent.

It is sometimes more convenient to express the side-leakage factor in equation (28) in terms of the radius of curvature ratio R_y/R_x instead of the ellipticity parameter k through the following relation:

$$k = 1.03\left(\frac{R_y}{R_x}\right)^{0.64} \tag{29}$$

where

$$\frac{1}{R_y} = \frac{1}{r_{Ay}} + \frac{1}{r_{By}} \tag{30}$$

$$\frac{1}{R_x} = \frac{1}{r_{Ax}} + \frac{1}{r_{Bx}} \tag{31}$$

Using equation (29) avoids the need to evaluate elliptic integrals of the first and second kinds in the determination of k. The minimum film thickness can thus be derived directly from a knowledge of the radii of curvature of the contacting bodies (r_{Ax}, r_{Bx}, r_{Ay}, and r_{By}).

It is interesting to compare the new, point-contact, minimum-film-thickness formula (eq. (28)) with the corresponding equation generated in the 1960's (ref. 7) for line contacts

$$H_{min,L} = 2.65\, U^{0.70} G^{0.54} W^{-0.13} \tag{32}$$

The powers of U, G, and W in equations (28) and (32) are quite similar considering the different numerical procedures upon which they are based. It is also worth noting that the power of W in equation (28) is extremely close to the value of -0.074 proposed by Archard and Cowking in their study of point contacts (ref. 8).

CENTRAL-FILM-THICKNESS FORMULA

There is interest in knowning the central film thickness, in addition to the minimum film thickness, in elastohydrodynamic contacts. The procedure used in obtaining the central film thickness was the same as that used in obtaining the minimum film thickness and is not repeated here. The central-film-thickness formula obtained from the results is

$$\tilde{H}_c = 2.69\, U^{0.67} G^{0.53} W^{-0.067} (1 - 0.61\, e^{-0.73k}) \tag{33}$$

Comparing the central-film-thickness formula (eq. (33)) with the minimum-film-thickness formula (eq. (28)) reveals a slight difference. In equation (33) the load exponent is small but negative, as it was for the minimum-film-thickness formula. This is in contrast with the recent numerical study of Ranger, et al. (ref. 9) who found a small but positive exponent on the dimensionless load W in their formulation of a central film

thickness.

Table VI gives the 34 different cases used to obtain equation (33). In this table, H_c corresponds to the central film thickness obtained from the EHL point-contact theory developed in reference 2, and $\tilde{H}_c$ corresponds to the central film thickness obtained from equation (33). The percentage difference between these two values is given by D_2 and is written as

$$D_2 = \left(\frac{\tilde{H}_c - H_c}{H_c}\right)100 \tag{34}$$

In table VI the values of D_2 are within ±10 percent.

CONCLUDING REMARKS

By using the procedures outlined by the authors in an earlier publication the influence of the ellipticity parameter and the dimensionless speed U, load W, and material G parameters on minimum film thickness has been investigated. The ellipticity parameter was varied from 1 (a ball-on-plate configuration) to 8 (a configuration approaching a line contact). The dimensionless speed parameter was varied over a range of nearly two orders of magnitude. The dimensionless load parameter was varied over a range of one order of magnitude. Situations equivalent to using solid materials of bronze, steel, and silicon nitride and lubricants of paraffinic and naphthenic mineral oils were considered in investigating the role of the dimensionless material parameter. Thirty-four different cases were used to generate the minimum-film-thickness and central-film-thickness relations:

$$\tilde{H}_{min} = 3.63\, U^{0.68} G^{0.49} W^{-0.073} (1 - e^{-0.68k})$$

$$\tilde{H}_c = 2.69\, U^{0.67} G^{0.53} W^{-0.067} (1 - 0.61\, e^{-0.73k})$$

It was found that the ellipticity parameter k can be written as

$$k = 1.03\left(\frac{R_y}{R_x}\right)^{0.64}$$

where R_y/R_x is the radius of curvature ratio.

Contour plots have been presented that indicate in detail the pressure distribution and the film thickness. In some solutions, pressure spikes were in evidence. The theo-

retical solutions of film thickness have all the essential features of previously reported experimental observations based upon optical interferometry.

The importance of the present report lies in the fact that it presents for the first time a complete theoretical film-thickness equation for elastohydrodynamic point contacts operating under fully flooded conditions. The exponents on the various dimensionless parameters governing minimum film thickness in such conjunctions are quite similar to those developed earlier by Dowson for line contacts. The most dominant exponent occurs in association with the speed parameter, while the exponent on the load parameter is very small and negative. The material parameter also carries a significant exponent, although the range of this parameter in engineering situations is limited. A central-film-thickness formula exists for the contact geometry of a ball on a plate from which an estimate can be made of the minimum film thickness. However, the formula presented herein is valid for any contact geometry and proceeds directly to the evaluation of the minimum film thickness.

Perhaps the most significant feature of the proposed minimum-film-thickness formula is that it can be applied to any contacting solids that present an elliptical Hertzian contact region. Many machine elements, particularly rolling-element bearings, possess such geometry. And it is expected that the new minimum-film-thickness formula will find application in such fields.

Lewis Research Center,
National Aeronautics and Space Administration,
Cleveland, Ohio, July 28, 1976,
505-04.

REFERENCES

1. Hamrock, Bernard J.; and Dowson, Duncan: Numerical Evaluation of the Surface Deformation of Elastic Solids Subjected to a Hertzian Contact Stress. NASA TN D-7774, 1974.

2. Hamrock, Bernard J.; and Dowson, Duncan: Isothermal Elastohydrodynamic Lubrication of Point Contacts. I - Theoretical Formulation. NASA TN D-8049, 1975; also J. Lub. Tech. (Trans. ASME, ser. F), vol. 98, Apr. 1976, pp. 223-229.

3. Hamrock, Bernard J.; and Dowson, Duncan: Isothermal Elastohydrodynamic Lubrication of Point Contacts. II - Ellipticity Parameter Results. NASA TN D-8166, 1976; also J. Lub. Tech. (Trans. ASME, ser. F), vol. 98, July 1976, pp. 375-383.

4. Roelands, C. J. A.: Correlational Aspects of the Viscosity-Temperature-Pressure Relationship of Lubricating Oils. Druk U. R. B., Groningen, The Netherlands, 1966.

5. Dowson, D.; and Higginson, G. R.: Elastohydrodynamic Lubrication. Pergamon Press, 1966.

6. Cameron, A.; and Gohar, R.: Theoretical and Experimental Studies of the Oil Film in Lubricated Point Contact. Proc. Royal Soc. (London), vol. 291A, no. 1427, Apr. 1966, pp. 520-536.

7. Dowson, D.: Elastohydrodynamics. Proc. Inst. Mech. Engrs., vol. 182, pt. 3A, 1968, pp. 151-167.

8. Archard, J. F.; and Cowking, E. W.: Elastohydrodynamic Lubrication of Point Contacts. Proc. Inst. Mech. Engrs., vol. 180, pt. 3B, 1965-1966, pp. 47-56.

9. Ranger, A. P.; Ettles, C. M. M.; and Cameron, A.: The Solution of the Point Contact Elasto-Hydrodynamic Problem. Proc. Royal Soc. (London), vol. 346A, no. 1645, Oct. 1975, pp. 227-244.

TABLE I. - EFFECT OF ELLIPTICITY PARAMETER ON MINIMUM FILM THICKNESS

Ellipticity parameter, k	Minimum film thickness		Difference between H_{min} and $\tilde{H}_{min}$, D_1, percent
	Obtained from EHL point-contact theory, H_{min}	Obtained from least-square fit, $\tilde{H}_{min}$	
1	3.367×10^{-6}	3.464×10^{-6}	+2.88
1.25	4.105	4.031	-1.80
1.5	4.565	4.509	-1.22
1.75	4.907	4.913	+.11
2	5.255	5.252	-.05
2.5	5.755	5.781	+.45
3	6.091	6.156	+1.08
4	6.636	6.613	-.34
6	6.969	6.961	-.12
8	7.048	7.050	+.02

TABLE II. - EFFECT OF DIMENSIONLESS SPEED PARAMETER ON MINIMUM FILM THICKNESS

Dimensionless speed parameter, U	Minimum film thickness		Difference between H_{min} and $\tilde{H}_{min}$, D_1, percent
	Obtained from EHL point-contact theory, H_{min}	Obtained from least-square fit, $\tilde{H}_{min}$	
0.08416×10^{-11}	3.926×10^{-6}	3.915×10^{-6}	-0.275
.1683	6.156	6.252	+1.564
.2525	8.372	8.223	-1.780
.3367	9.995	9.987	-.078
.4208	11.61	11.61	-.004
.5892	14.39	14.57	+1.280
.8416	18.34	18.54	+1.104
1.263	24.47	24.39	-.320
1.683	29.75	29.61	-.467
2.104	34.58	34.43	-.432
2.525	39.73	38.95	-1.977
2.946	43.47	43.22	-.576
3.367	47.32	47.30	-.042
4.208	54.57	54.99	+.765
5.050	61.32	62.20	+1.430

TABLE III. - EFFECT OF DIMENSIONLESS LOAD PARAMETER

ON MINIMUM FILM THICKNESS

Dimensionless load parameter, W	Minimum film thickness		Difference between H_{min} and $\tilde{H}_{min}$, D_1, percent
	Obtained from EHL point-contact theory, H_{min}	Obtained from least-square fit, $\tilde{H}_{min}$	
0.1106×10^{-6}	6.969×10^{-6}	6.941×10^{-6}	-0.41
.2211	6.492	6.599	+1.65
.3686	6.317	6.358	+.64
.5528	6.268	6.172	-1.52
.7371	6.156	6.044	-1.81
.9214	6.085	5.947	-2.27
1.106	5.811	5.868	+.98
1.290	5.657	5.803	+2.58

TABLE IV. - EFFECT OF SOLID MATERIAL AND LUBRICANT AS REPRESENTED IN DIMENSIONLESS

MATERIAL PARAMETER ON MINIMUM FILM THICKNESS

Solid material	Lubricant	Dimensionless material parameter, G	Dimensionless speed parameter, U	Dimensionless load parameter, W	Minimum film thickness		Difference between H_{min} and $\tilde{H}_{min}$, D_1, percent
					Obtained from EHL point-contact theory, H_{min}	Obtained from least-square fit, $\tilde{H}_{min}$	
Bronze	Paraffinic	2310	0.3296×10^{-11}	0.7216×10^{-6}	6.931×10^{-6}	6.873×10^{-6}	-0.84
Bronze	Naphthenic	3591	.9422	.7216	17.19	17.404	+1.25
Steel	Paraffinic	4522	.1683	.3686	6.317	6.336	+.31
Silicon nitride	Paraffinic	6785	.1122	.2456	6.080	6.038	-.70

TABLE V. - DATA SHOWING EFFECT OF ELLIPTICITY, LOAD, SPEED, AND MATERIAL ON MINIMUM FILM THICKNESS

Case	Ellipticity parameter, k	Dimensionless load parameter, W	Dimensionless speed parameter, U	Dimensionless material parameter, G	Minimum film thickness		Difference between H_{min} and $\tilde{H}_{min}$, D_1, percent	Results
					Obtained from EHL point-contact theory, H_{min}	Obtained from least-square fit, $\tilde{H}_{min}$		
1	1	0.1106×10^{-6}	0.1683×10^{-11}	4522	3.367×10^{-6}	3.514×10^{-6}	+4.37	Ellipticity
2	1.25	↓	↓	↓	4.105	4.078	-.66	
3	1.5				4.565	4.554	-.24	
4	1.75				4.907	4.955	+.98	
5	2				5.255	5.294	+.74	
6	2.5				5.755	5.821	+1.15	
7	3				6.091	6.196	+1.72	
8	4				6.636	6.652	+.24	
9	6				6.969	7.001	+.46	
10	8	↓	↓	↓	7.048	7.091	+.61	
11	6	.2211	↓	↓	6.492	6.656	+2.53	Load plus case 9
12	↓	.3686			6.317	6.412	+1.50	
13		.5528			6.268	6.225	-.69	
14		.7371			6.156	6.095	-.99	
15		.9214			6.085	5.997	-1.45	
16		1.106			5.811	5.918	+1.84	
17		1.290	↓		5.657	5.851	+3.43	
18		.7371	.08416		3.926	3.805	-3.08	Speed plus case 14
19		↓	.2525		8.372	8.032	-4.06	
20			.3367		9.995	9.769	-2.26	
21			.4208		11.61	11.37	-2.07	
22			.5892		14.39	14.29	-.69	
23			.8416		18.34	18.21	-.71	
24			1.263		24.47	24.00	-1.92	
25			1.683		29.75	29.18	-1.92	
26			2.104		34.58	33.96	-1.79	
27			2.525		39.73	38.44	-3.25	
28			2.946		43.47	42.69	-1.79	
29			3.367		47.32	46.76	-1.18	
30			4.208		54.57	54.41	-.29	
31			5.050	↓	61.32	61.59	+.44	
32		.7216	.3296	2310	6.931	6.938	+.10	Materials plus case 9
33		.7216	.9422	3491	17.19	17.59	+2.33	
34	↓	.2456	.1122	6785	6.080	6.116	+.59	

TABLE VI. - DATA SHOWING EFFECT OF ELLIPTICITY, LOAD, SPEED, AND MATERIAL ON CENTRAL FILM THICKNESS

Case	Ellipticity parameter, k	Dimensionless load parameter, W	Dimensionless speed parameter, U	Dimensionless material parameter, G	Central film thickness		Difference between H_c and $\tilde{H}_c$, D_2, percent	Results
					Obtained from EHL point-contact theory, H_c	Obtained from least-square fit, $\tilde{H}_c$		
1	1	0.1106×10^{-6}	0.1683×10^{-11}	4522	6.860×10^{-6}	6.215×10^{-6}	-9.40	
2	1.25	↓	↓	↓	6.964	6.647	-4.55	
3	1.5				7.001	7.006	+.07	
4	1.75				7.015	7.306	+4.15	
5	2				7.402	7.556	+2.08	Ellipticity
6	2.5				7.653	7.937	+3.71	
7	3				7.845	8.202	+4.55	
8	4				8.292	8.513	+2.67	
9	6				8.657	8.736	+.91	
10	8	↓			8.672	8.787	+1.33	
11	6	.2211			7.796	8.339	+6.97	
12		.3686			7.505	8.059	+7.38	
13		.5528			7.309	7.843	+7.31	
14		.7371			7.517	7.693	+2.34	Load plus case 9
15		.9214			7.611	7.578	-.43	
16		1.106			7.416	7.487	+.96	
17		1.290	↓		6.762	7.410	+9.58	
18		.7371	.08416		4.917	4.836	-1.65	
19			.2525		9.999	10.10	+1.01	
20			.3367		11.40	12.24	+7.37	
21			.4208		13.07	14.21	+8.72	
22			.5892		17.13	17.81	+3.97	
23			.8416		21.35	22.61	+5.90	
24			1.263		29.62	29.68	+.20	Speed plus case 14
25			1.683		35.50	35.98	+1.35	
26			2.104		41.05	41.79	+1.80	
27			2.525		46.64	47.22	+1.24	
28			2.946		51.08	52.36	+2.51	
29			3.367		55.56	57.26	+3.06	
30			4.208		63.81	66.49	+4.20	
31			5.050	↓	71.25	75.13	+5.45	
32		.7216	.3296	2310	8.422	8.466	:.52	Materials plus case 9
33		.7216	.9422	3591	20.70	21.62	+4.44	
34	↓	.2456	.1122	6785	7.825	7.825	0	

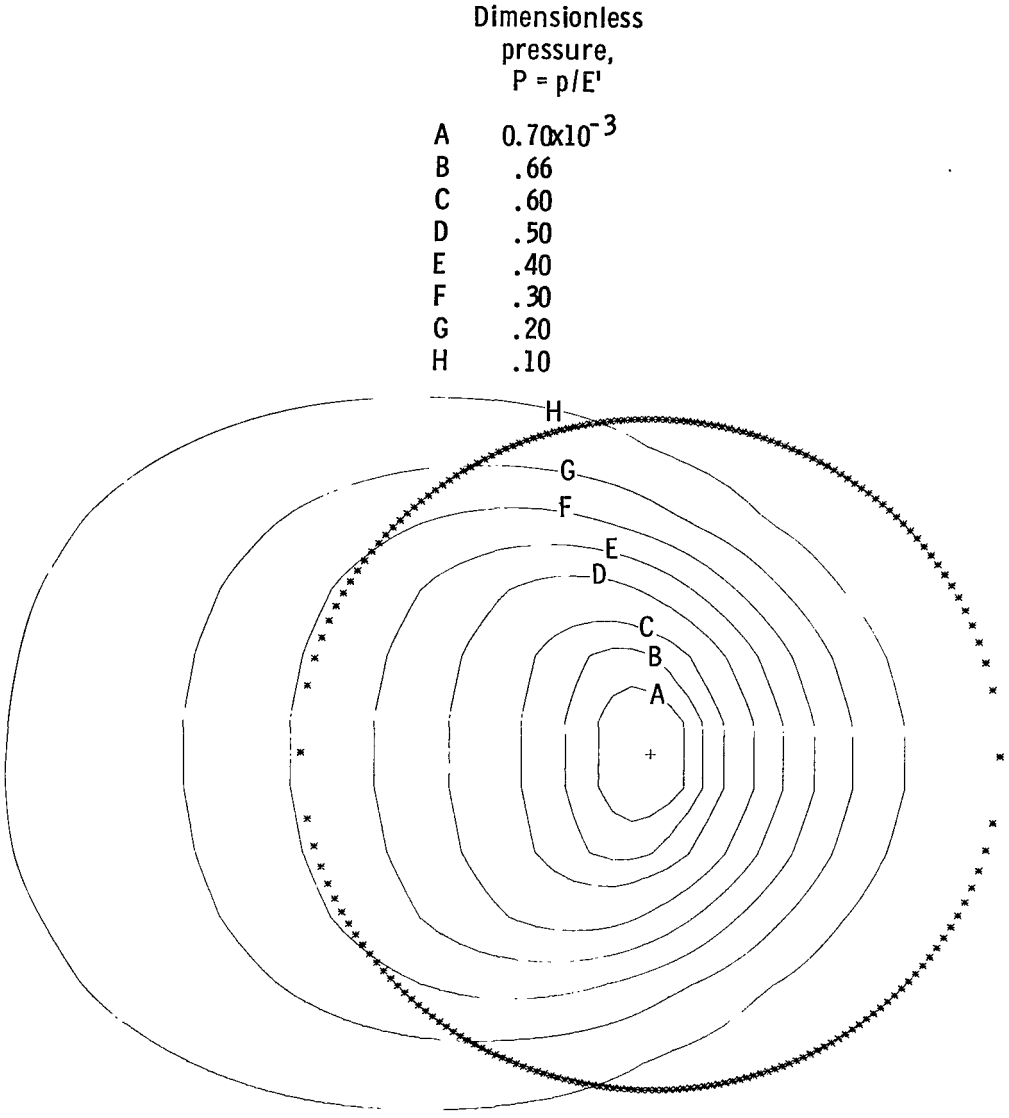

(a) k = 8.

Figure 1. Contour plots of dimensionless pressure for ellipticity parameters k of 8 and 1.25, respectively. The dimensionless parameters U, W, and G are held constant as defined in equation (7).

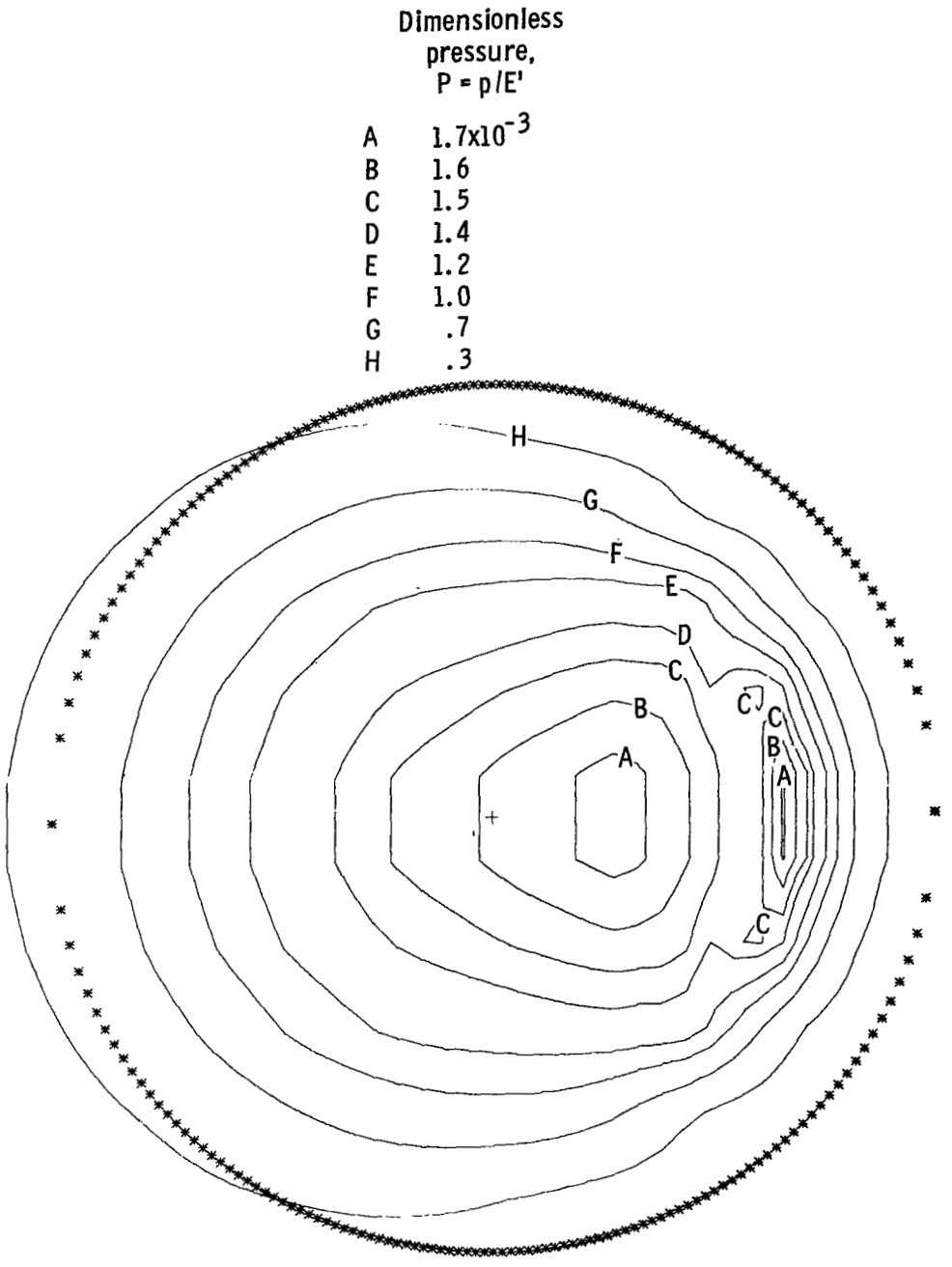

(b) k = 1.25.

Figure 1. - Concluded.

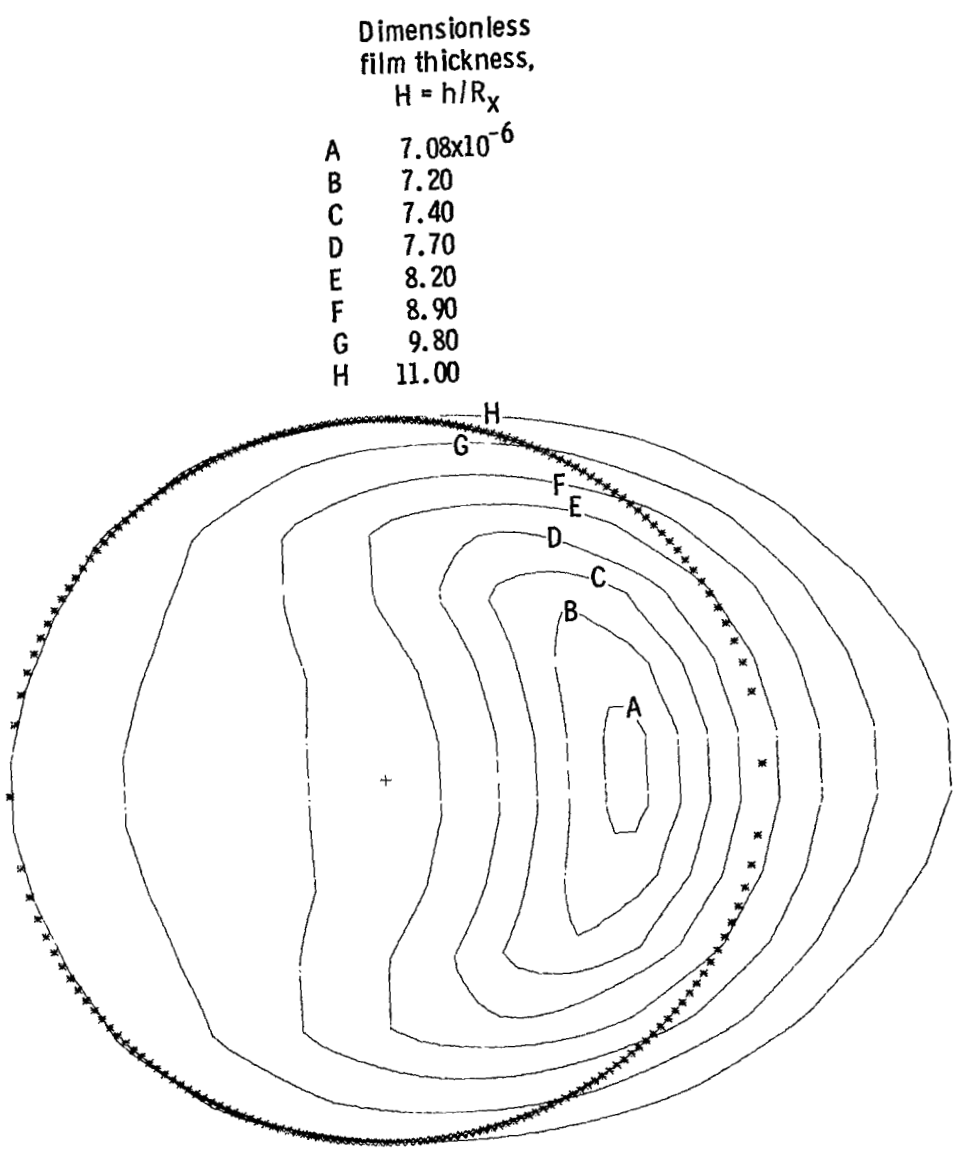

(a) k = 8.

Figure 2. - Contour plots of dimensionless film thickness for ellipticity parameters k of 8 and 1.25, respectively. The dimensionless parameters U, W, and G are held constant as defined in equation (7).

	Dimensionless film thickness, $H = h/R_x$
A	4.3×10^{-6}
B	4.6
C	5.0
D	5.5
E	6.0
F	6.6
G	7.4
H	8.2

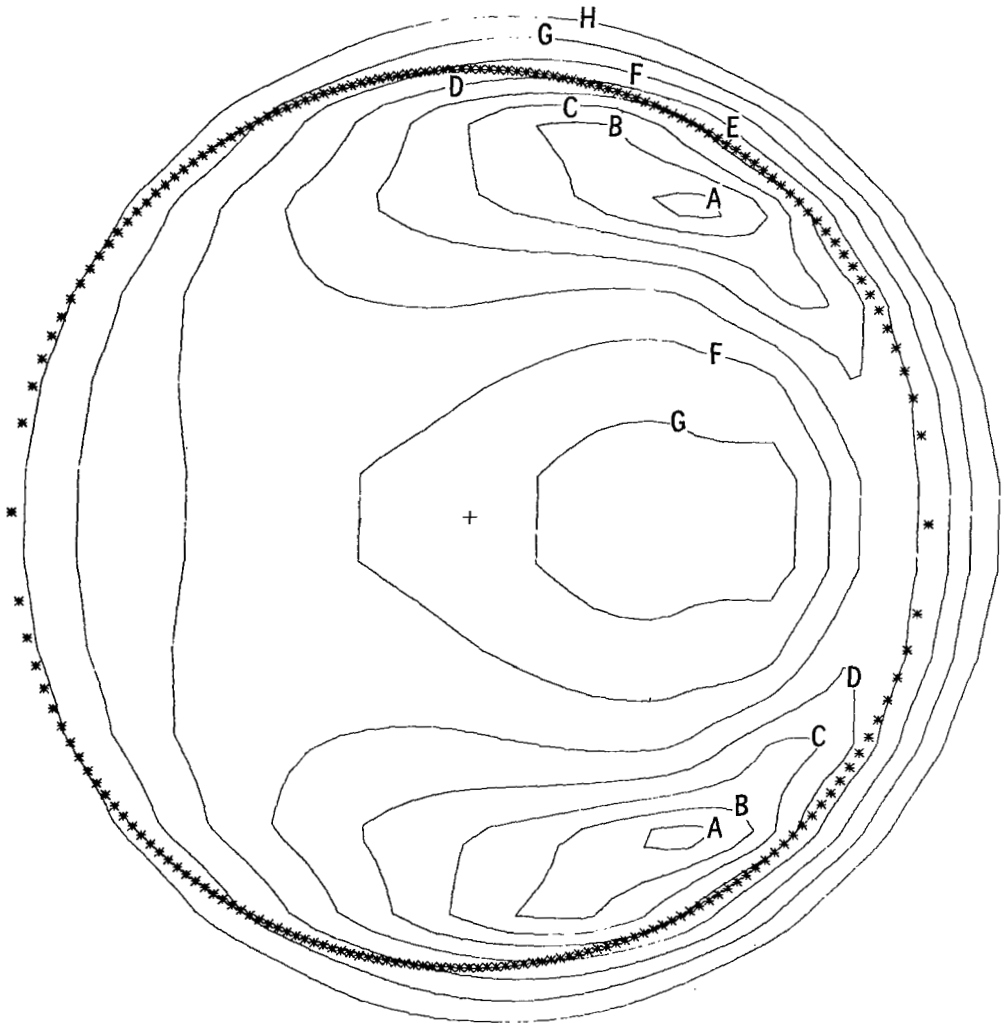

(b) k = 1.25.

Figure 2. - Concluded.

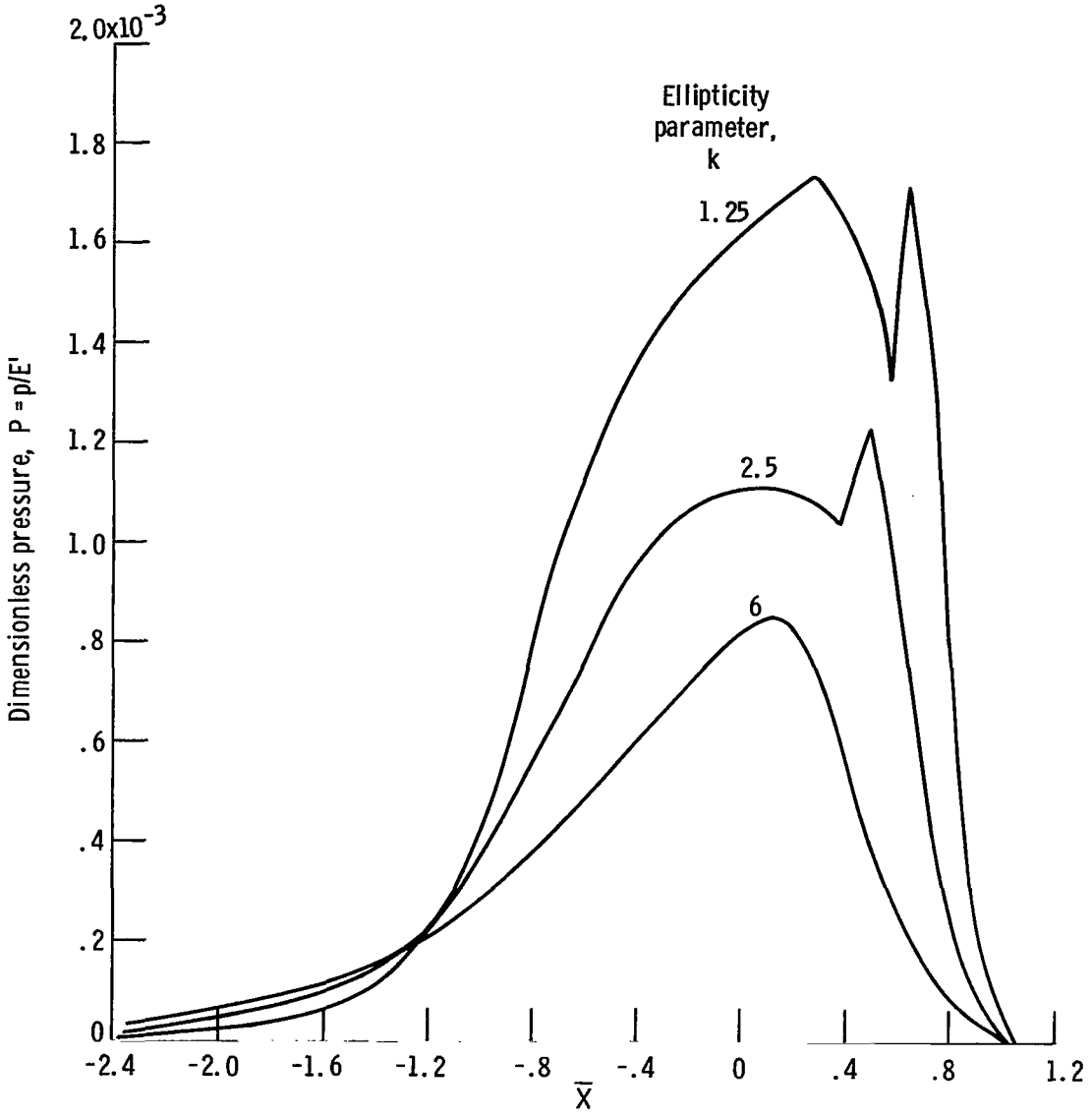

(a) Dimensionless pressure.

Figure 3. - Variation of dimensionless pressure and film thickness on $\bar{X}$-axis for three values of ellipticity parameter. The value of $\bar{Y}$ is held fixed near axial center of contact.

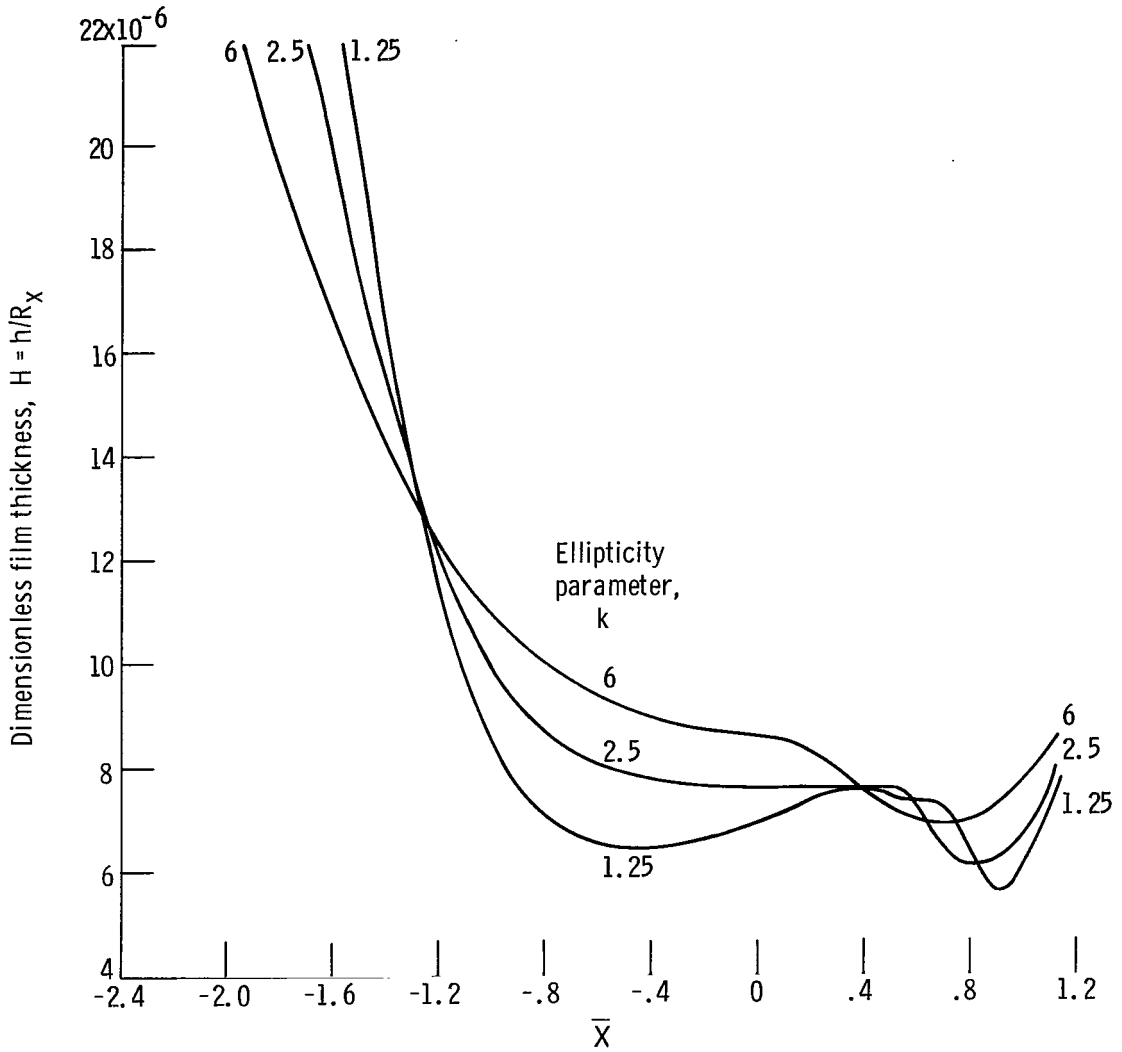

(b) Dimensionless film thickness.

Figure 3. - Concluded.

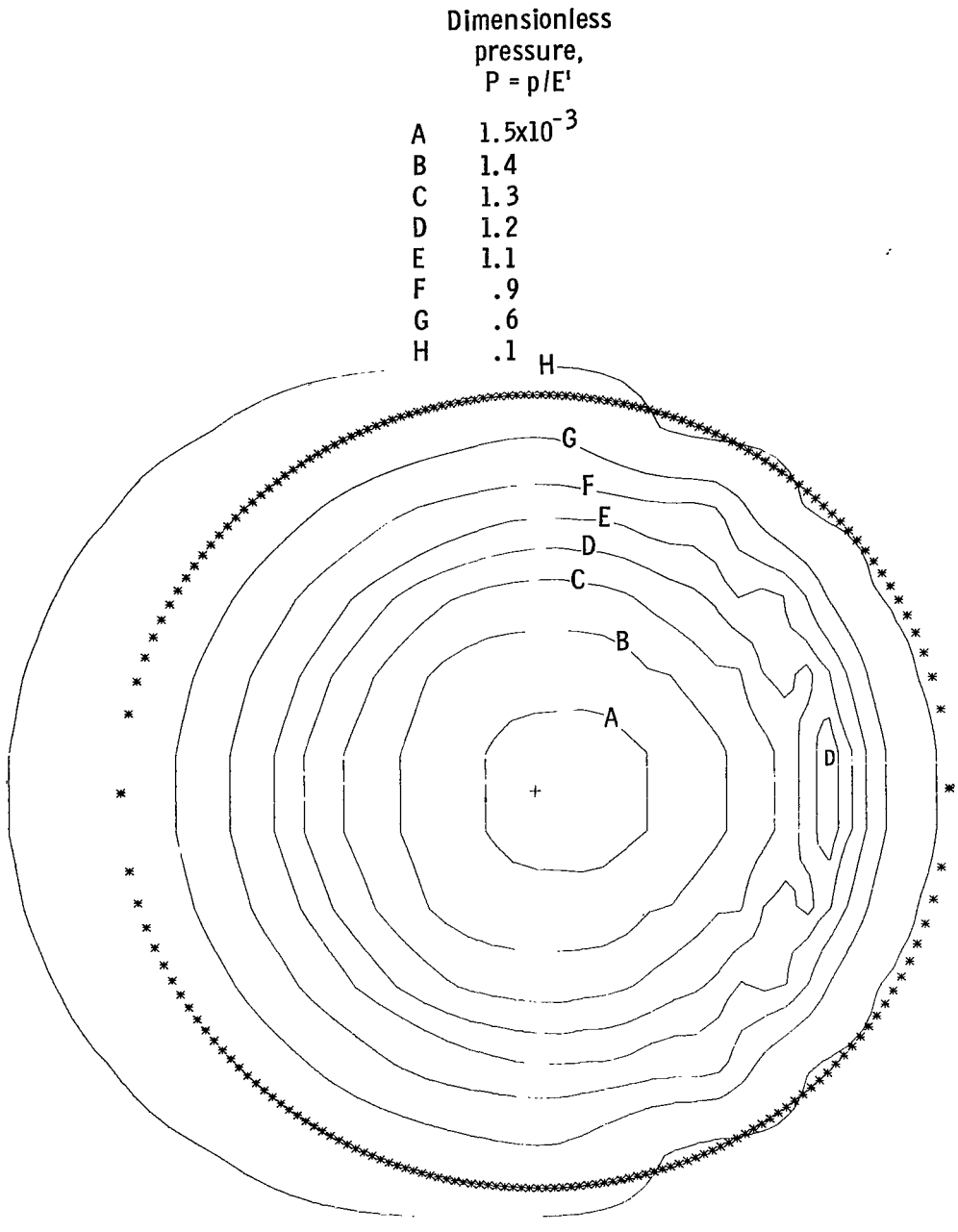

(a) $U = 0.8416 \times 10^{-12}$.

Figure 4. - Contour plots of dimensionless pressure for dimensionless speed parameters U of 0.8416×10^{-12} and 0.5050×10^{-10}, respectively. The dimensionless parameters k, W, and G are held constant as defined in equation (13).

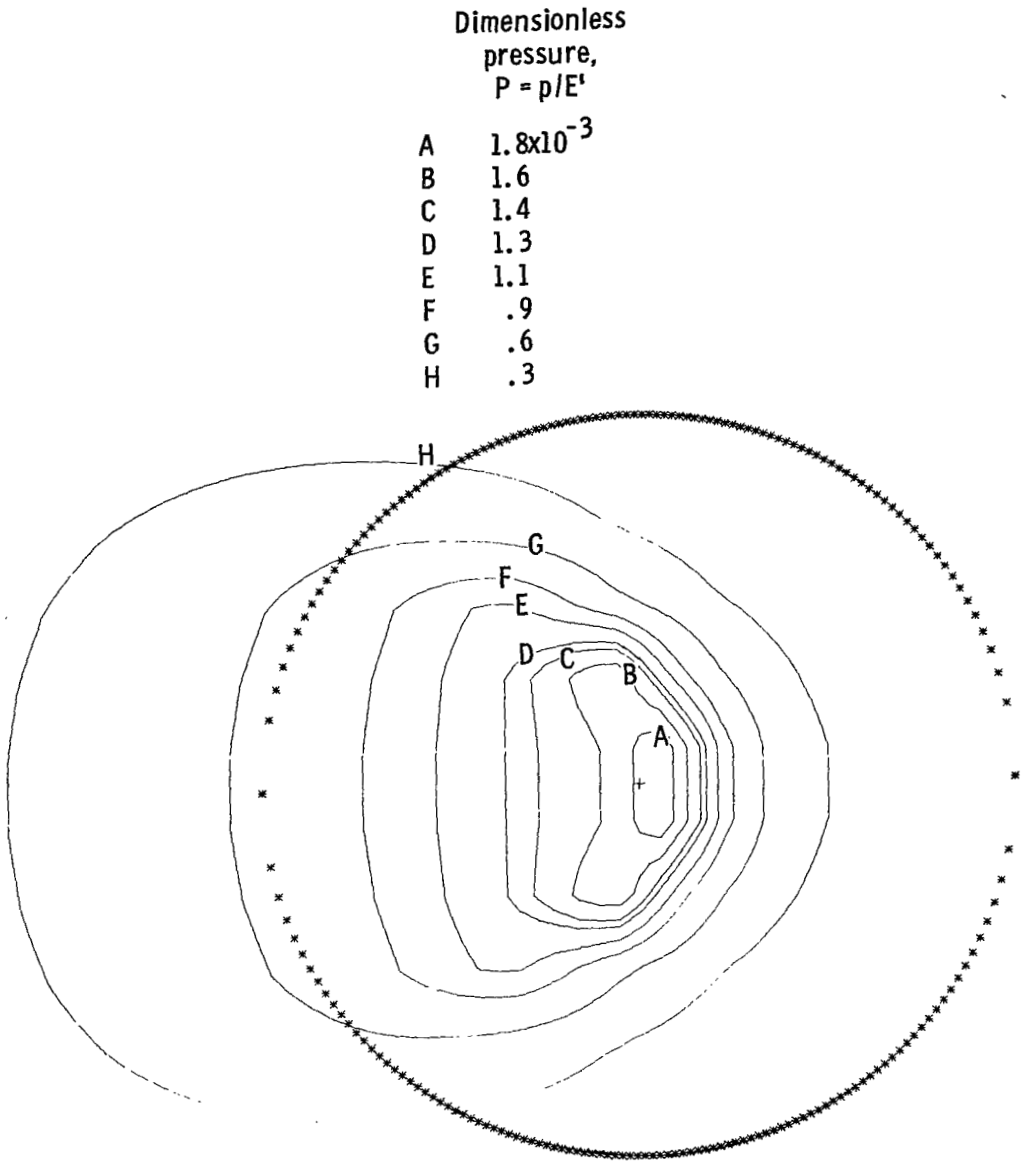

(b) U = 0.5050×10^{-10}.

Figure 4. - Concluded.

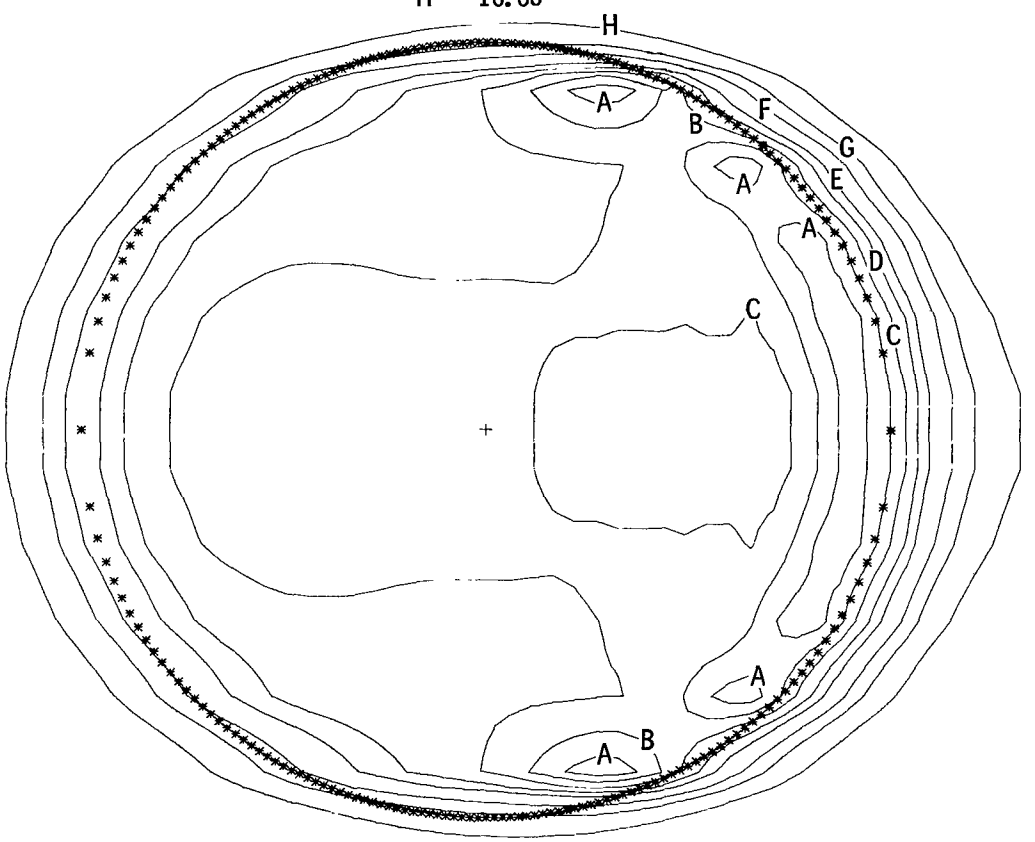

(a) $U = 0.8416 \times 10^{-12}$.

Figure 5. - Contour plots of dimensionless film thickness for dimensionless speed parameters U of 0.8416×10^{-12} and 0.5050×10^{-10}. The dimensionless parameters k, W, and G are held constant as defined in equation (13).

	Dimensionless film thickness, $H = h/R_x$
A	61.4×10^{-6}
B	62.0
C	63.0
D	65.0
E	68.0
F	72.0
G	78.0
H	86.0

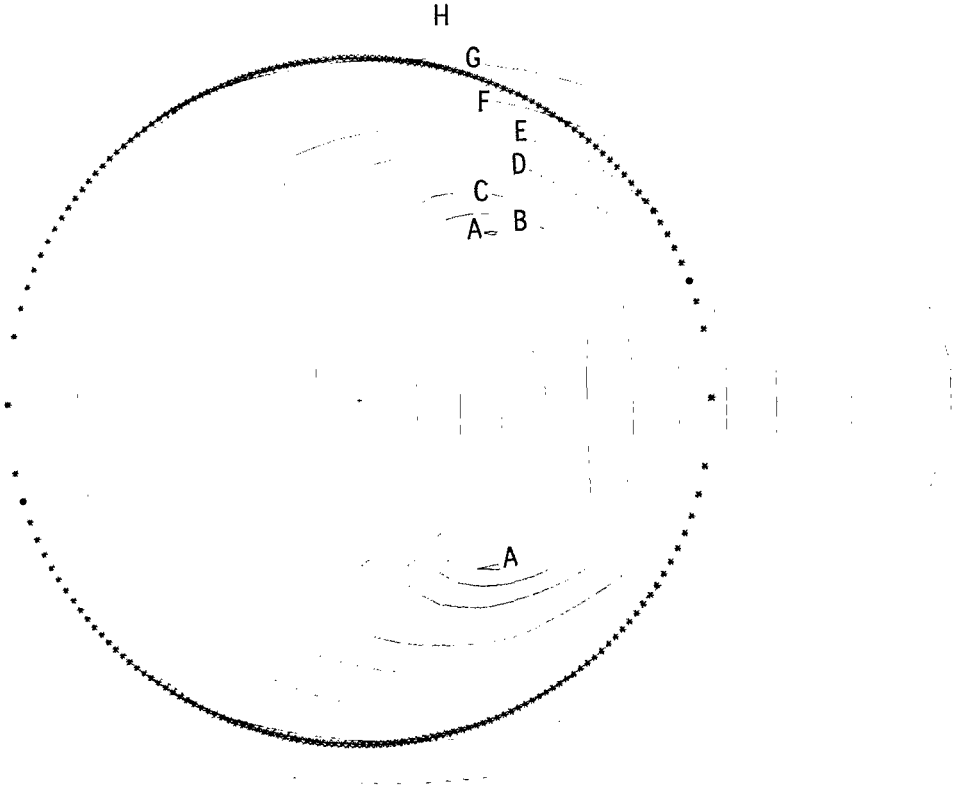

(b) $U = 0.5050 \times 10^{-10}$.

Figure 5. - Concluded.

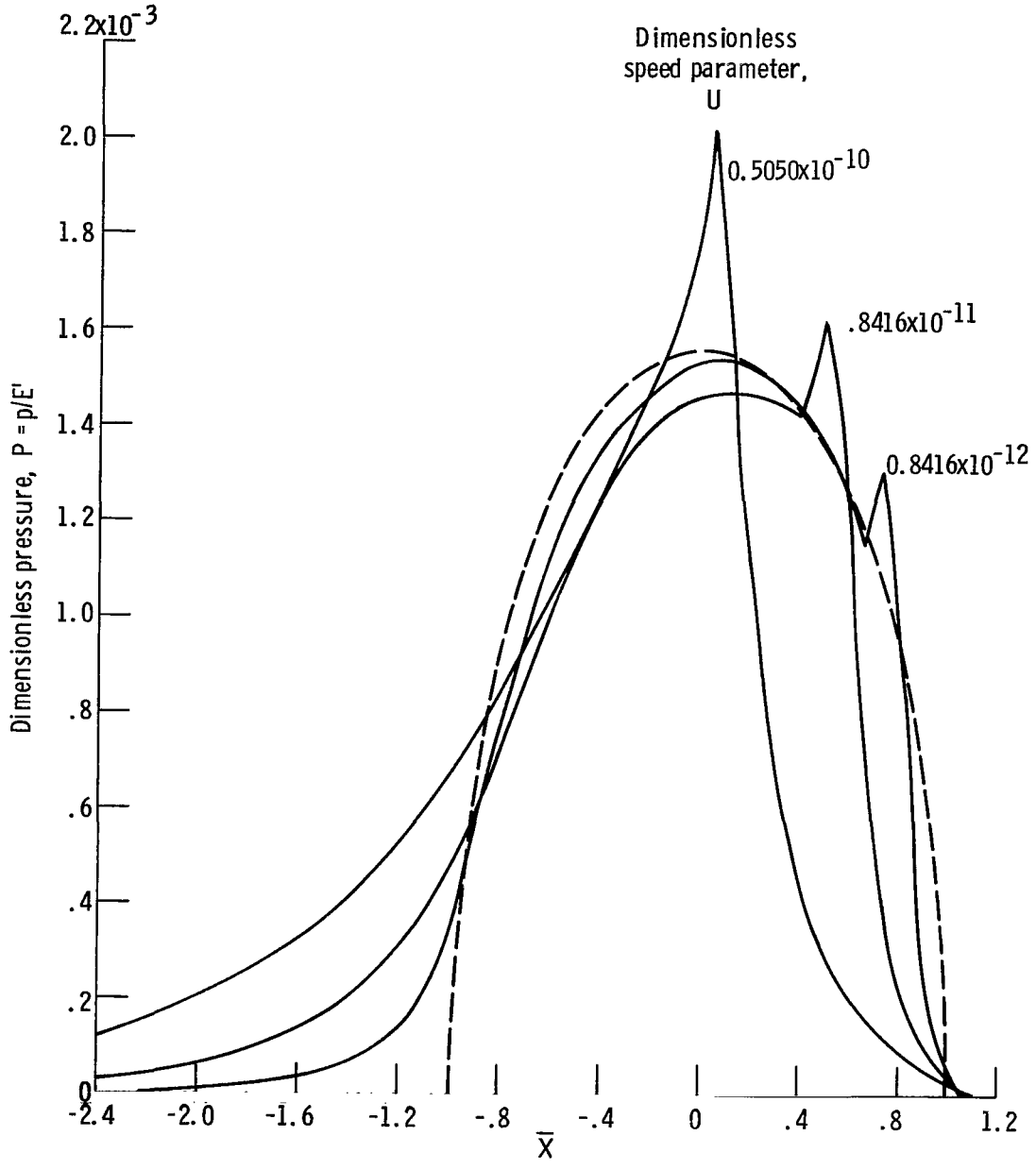

(a) Dimensionless film thickness.

Figure 6. - Variation of dimensionless pressure and film thickness on $\bar{X}$-axis for three values of dimensionless speed parameter. The value of $\bar{Y}$ is held fixed near axial center of contact.

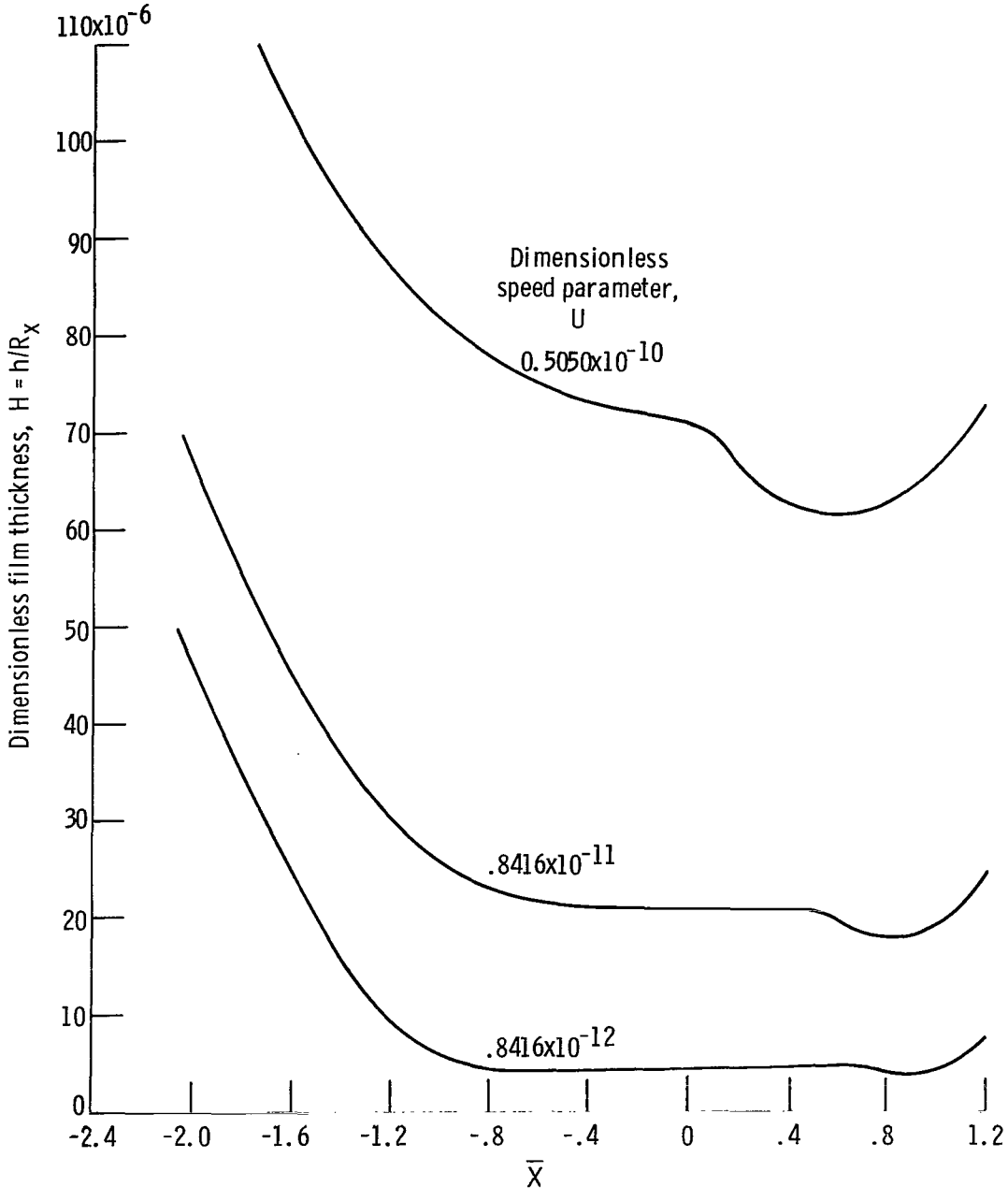

(b) Dimensionless film thickness.

Figure 6. - Concluded.

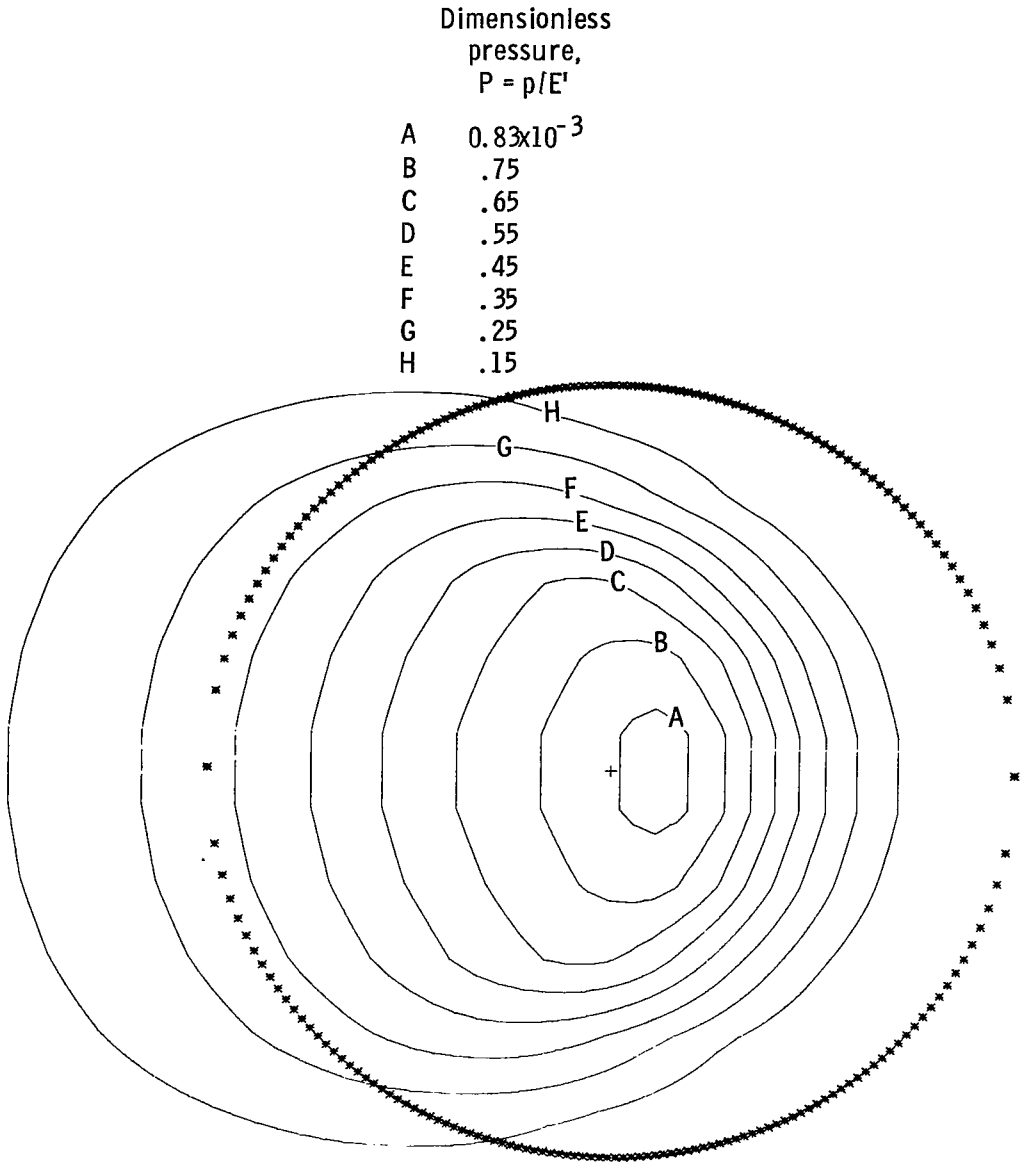

(a) $W = 0.1106 \times 10^{-6}$.

Figure 7. - Contour plots of dimensionless pressure for dimensionless load parameters W of 0.1106×10^{-6} and 0.1290×10^{-5}, respectively. The dimensionless parameters k, U, and G are held constant as defined in equation (18).

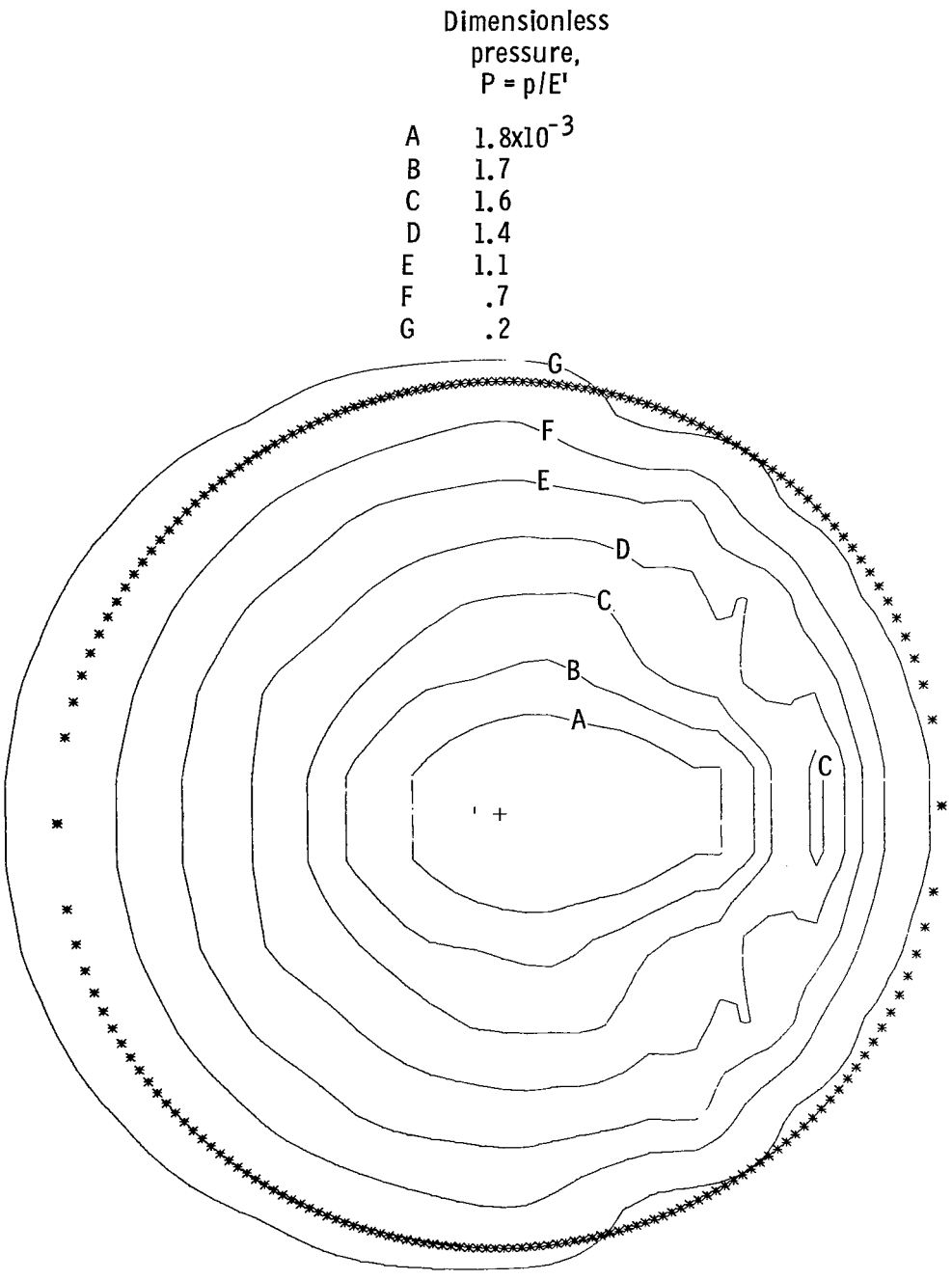

(b) W = 0.1290×10^{-5}.

Figure 7. - Concluded.

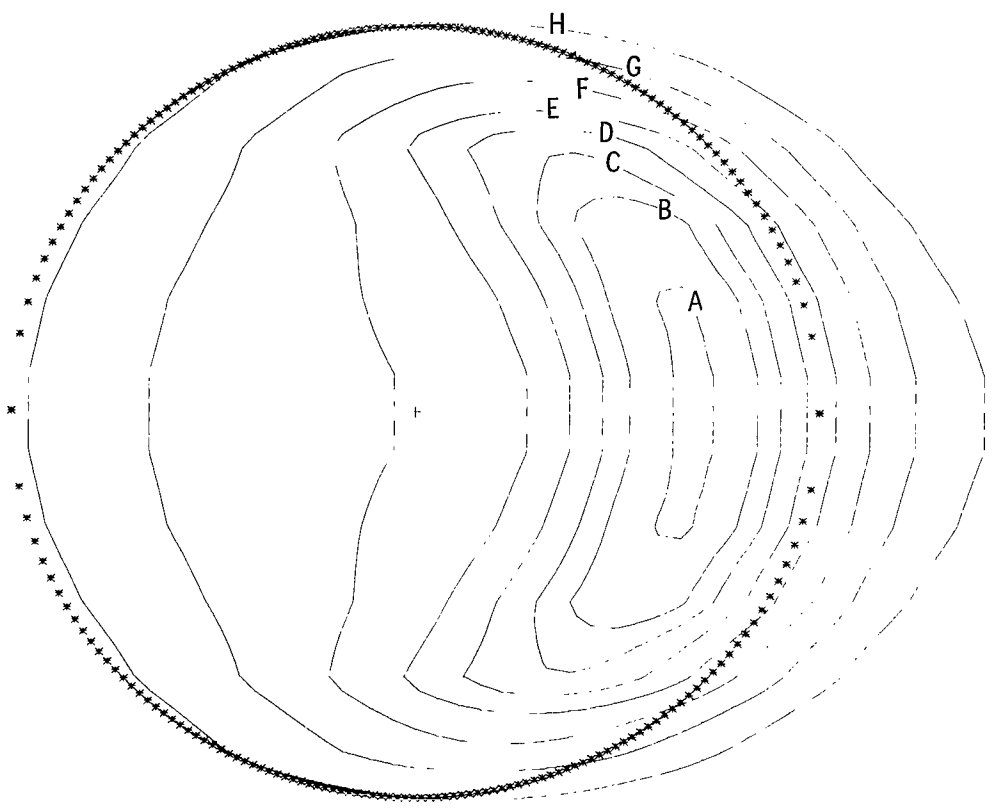

(a) $W = 0.1106 \times 10^{-6}$.

Figure 8. - Contour plots of dimensionless film thickness for dimensionless load parameters W of 0.1106×10^{-6} and 0.1290×10^{-5}, respectively. The dimensionless parameters k, W, and G are held constant as defined in equation (18).

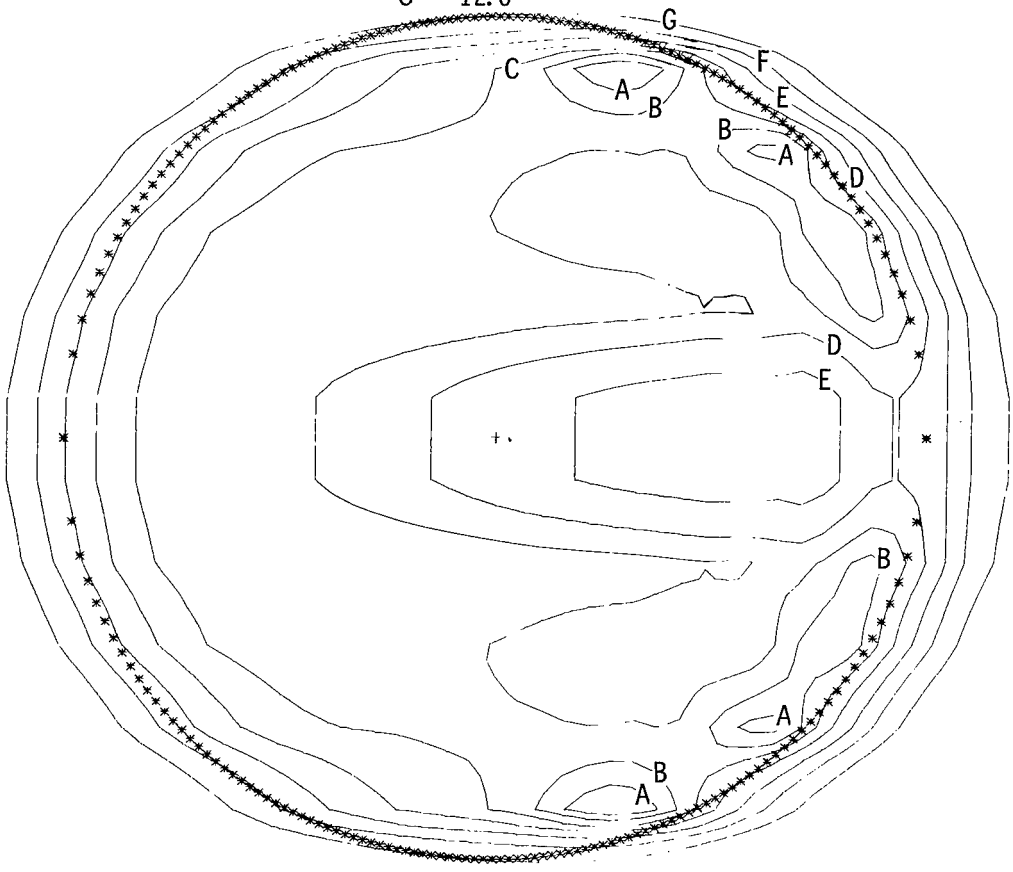

(b) W = 0.1290×10^{-5}.

Figure 8. - Concluded.

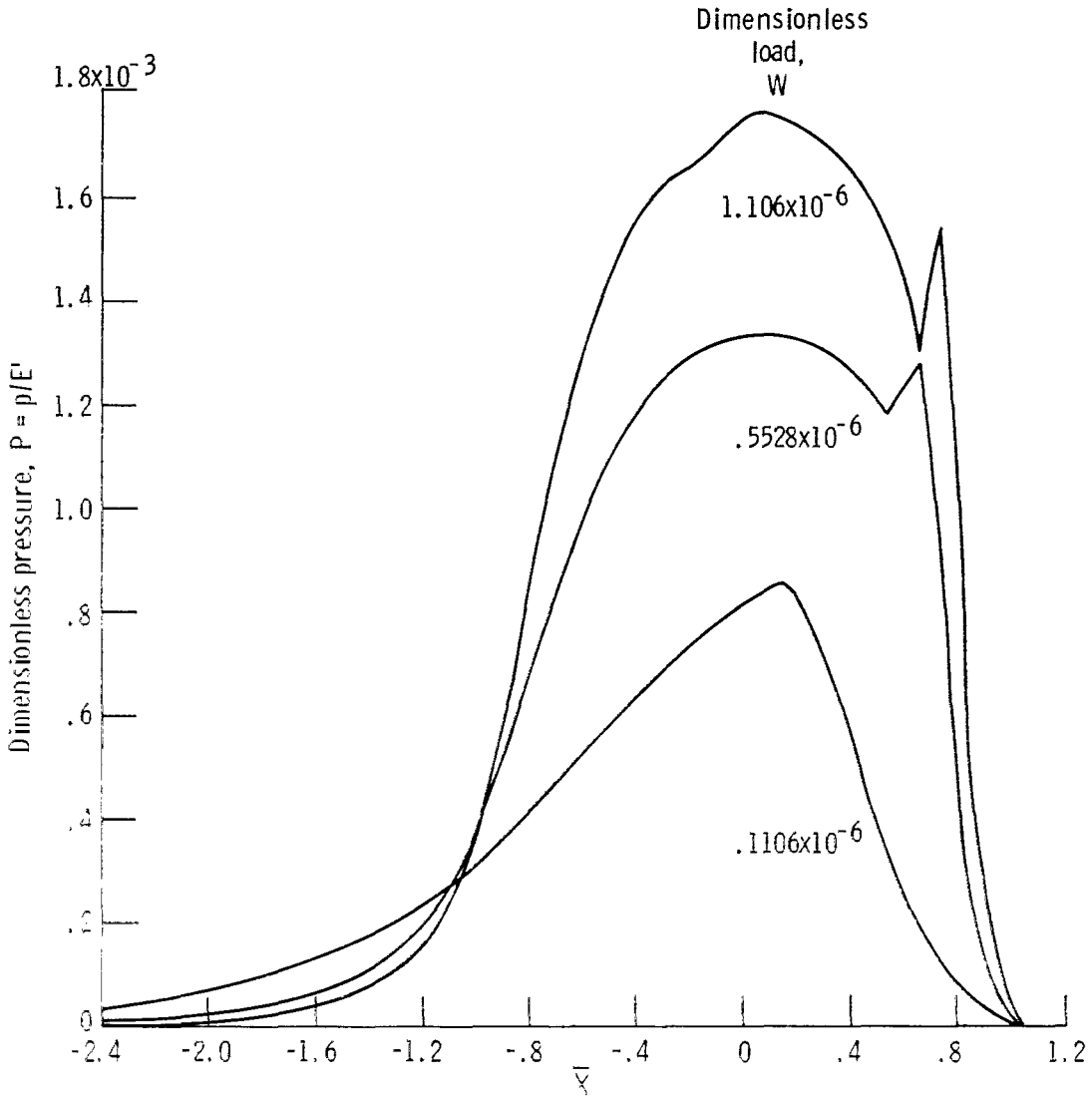

(a) Dimensionless pressure.

Figure 9. - Variation of dimensionless pressure and film thickness on $\bar{X}$-axis for three values of dimensionless load parameter. The value of $\bar{Y}$ is held fixed near axial center of contact.

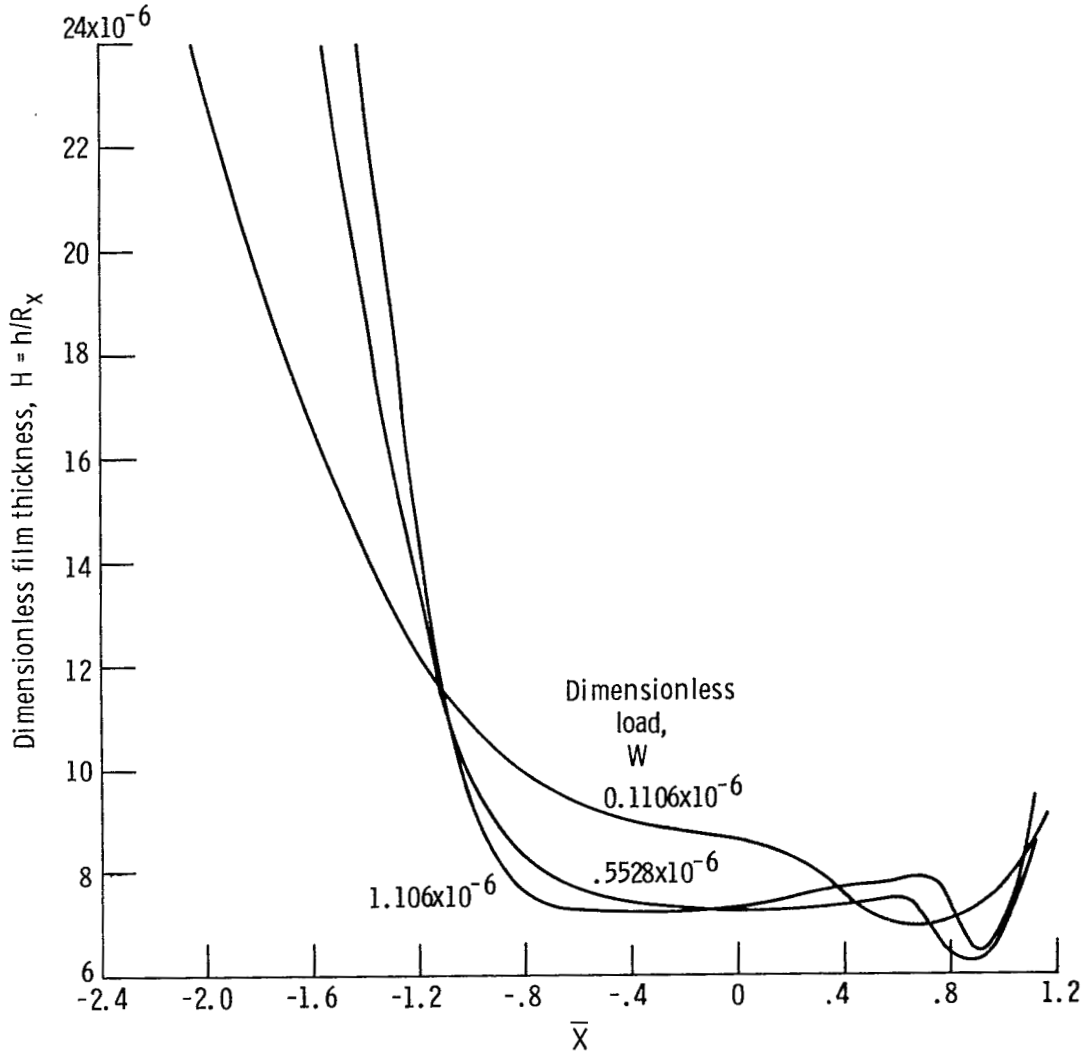

(b) Dimensionless film thickness.

Figure 9. - Concluded.

NASA-Langley, 1978 E-8712